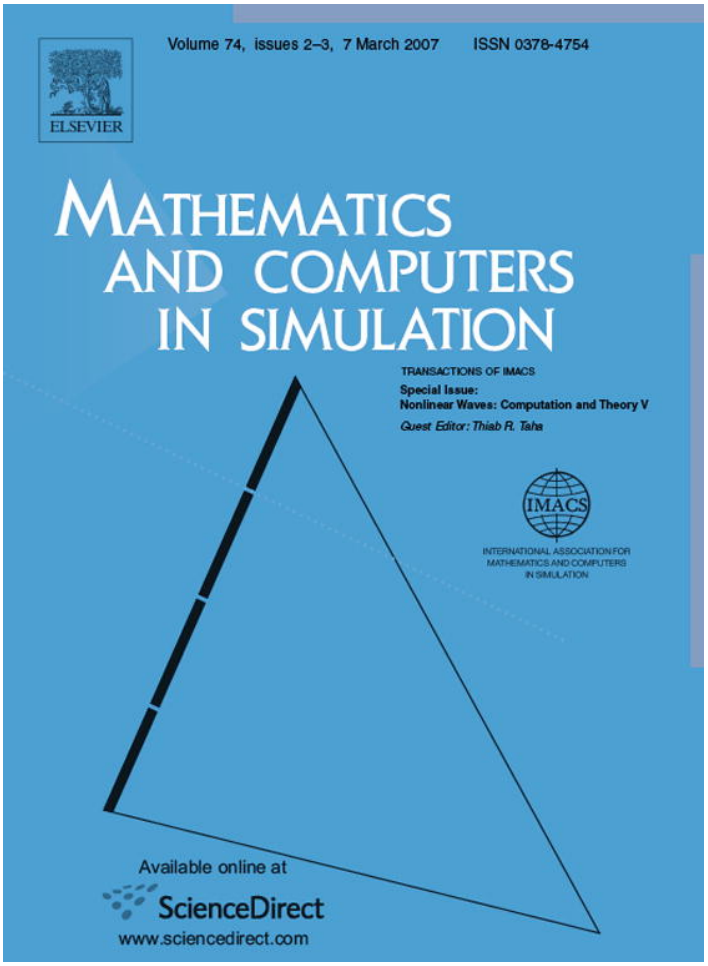

Available online at www.sciencedirect.com
ScienceDirect
Mathematics and Computers in Simulation 74 (2007) 203–213
MATHEMATICS AND COMPUTERS IN SIMULATION
www.elsevier.com/locate/matcom

Non-linear waves of the steady natural convection in a vertical fluid layer: A numerical approach

X.-H. Tang, C.I. Christov*

Department of Mathematics, University of Louisiana at Lafayette, Lafayette, LA 70504, USA

Available online 4 December 2006

Abstract

A fully implicit finite difference scheme is developed for the stream function formulation of unsteady thermoconvective flows. An artificial time is added in the equation for the stream function rendering it into an ultra-parabolic type. For each time stage of the real time, a convergence is obtained with respect to artificial time ("internal iterations"). An implicit efficient operator-splitting time stepping is designed and proved to be absolutely stable. Employing a conservative central-difference approximation of the non-linear terms makes the scheme absolutely stable without using upwind differences. As a result, the scheme has no scheme viscosity and has virtually negligible phase error, which makes it a useful tool for investigating the intricate structure of the thermoconvective flow. The scheme is second-order approximation both in time and space.

By means of the scheme developed, the convective flow in a vertical slot with differentially heated walls and vertical temperature gradient is studied for very large Rayleigh numbers. The model involves Boussinesq approximation and consists of a coupled system of a fourth-order in space equation for the stream function and a convection–diffusion equation for the temperature. The numerical results show that with increasing stratification parameter, the mode of the instability changes from traveling-wave to stationary-wave, which is consistent with the predictions of the linear theory of hydrodynamic instability. The role of the dimensionless wavelength is investigated and the issue of most dangerous wave is addressed numerically.

Keywords: G-jitter; Instability; Thermoconvection; Operator Spliiting; Implcit Schemes for Navier-Stokes

1. Introduction

Application of the operator-splitting methods for solving biharmonic equations began in [9] where the Douglas [10] scheme of "stabilizing correction" was applied to a parabolic equation containing first-order time derivative and the biharmonic spatial operator. Because of slower convergence in comparison with the second-order in space diffusion equations, the scheme [9] did not receive much attention. Recently, we have shown the way to radically accelerate the convergence of the splitting scheme for biharmonic equation [16,17]. Despite the perceived slow convergence, the operator splitting for fourth-order equations was still much faster than a direct implicit scheme, and was applied to lid-driven cavity flow of viscous liquid in [6] and allowed obtaining results for very large Reynolds numbers. Later on, in [5], a similar algorithm formed the basis of a special scheme satisfying Lyapunov functional for another kind of higher-order diffusion equation, called Swift–Hohenberg equation. Once again, the numerical effectiveness of the splitting method proved to be crucial in obtaining results for times, longer than any other work in literature.

* Corresponding author. Tel.: +1 337 482 5273; fax: +1 337 482 5346.
E-mail address: christov@louisiana.edu (C.I. Christov).

0378-4754/$32.00 © 2006 IMACS. Published by Elsevier B.V. All rights reserved.
doi:10.1016/j.matcom.2006.10.026

However, in case of physically unsteady Navier–Stokes equations, the fourth-order equation for the stream function is not of parabolic type because the time dependence enters via the time derivative of the Laplacian of stream function rather than the time derivative of stream function. This makes the straightforward application of operator splitting impossible. A way to apply operator splitting to stream function was proposed in [7] where a derivative with respect to an artificial time was added in the stream function equation making the latter of ultra-parabolic type. Such an approach benefits the algorithm twofold. First, it enables splitting which speeds up the calculations of a single time step by orders of magnitude. Second, the non-linear advective terms can be approximated in fully implicit fashion with respect to the physical time, after the time stepping with respect to the artificial time reaches convergence. Recently, we have addressed the stability issues of the scheme with artificial time in [8]. The modifications of the non-linear term proposed in [8] allowed us to prove the unconditional stability of the internal iterations.

The scheme with internal iterations [7] was further developed in [4] to model thermoconvective flows when a parabolic equation for the temperature is coupled to the equation for stream function. A second-order approximation in the real time was achieved there by means of staggering of the time grids for the two unknown functions. Although strongly implicit, the scheme in [4] is not unconditionally stable. A crucial element is the highly efficient solver for multidiagonal systems developed in [3]. The present work is a further development of the numerical tool created in [4] for thermoconvective flows in which the advances made in [8] are incorporated and an absolutely stable scheme is created.

The new scheme is applied to the thermoconvective flow in a vertical slot which is driven by the combination of the imposed horizontal and vertical temperature gradient and the buoyancy of the fluid. This flow was studied both experimentally and theoretically by Elder [11], who observed the transition from one-dimensional flow to a sequence of two-dimensional steady flows consisting of stacked vertical convection cells which were approximately periodic along the vertical axis in regions removed from the top and bottom of the slot. The linear stability analysis of this flow was carried out in [2] in a similar vein as for the vertical buoyant boundary layer [13]. The non-linear problem is much harder to treat, especially when gravity modulations are present (see [12,4]). This warrants the numerical approach which is the object of the present work.

2. Natural convective flow in a vertical slot

Consider the flow in a vertical slot with a linear vertical temperature gradient and differentially heated walls, as shown in Fig. 1. The following dimensionless variables are introduced:

$$x = \frac{x^*}{L}, \qquad y = \frac{y^*}{L}, \qquad \omega = \omega^* \frac{L^2}{\kappa}, \qquad t = t^* \frac{\kappa}{L^2}, \qquad \psi = \frac{\psi^*}{\nu}, \qquad \theta = \frac{T^* - T_\mathrm{m}}{\delta T} - \tau_B y,$$

$$\tau_B = \frac{\tau_B^* L}{\delta T}, \qquad Ra = \frac{\beta g_0 \delta T L^3}{\nu\kappa}, \qquad Pr = \frac{\nu}{\kappa}, \qquad 4\gamma^4 = \tau_B Ra.$$

The notation is standard: ν is the kinematic viscosity, κ the thermal diffusivity, L the width of the slot, T_0 is the temperature of the left wall at the cross-section $y = 0$, and δT the horizontal temperature difference, and quantities without an asterisk are dimensionless. Note that the temperature of the left wall is $T_\mathrm{l}^* = T_0 + \tau_B^* y^*$, while at the right wall it is $T_\mathrm{r}^* = T_0 - \delta T + \tau_B^* y^*$. We use the temperature in the middle, $T^*(x^* = L/2, y^* = 0) = T_\mathrm{m} \equiv T_0 - (1/2)\Delta T$ as the reference value of the temperature. Note that we have already determined here that the left wall is the warmer one, and from now on, we can assume that $\Delta T > 0$. Respectively, the dimensionless field $\theta(x, y, t)$ is the departure from a linear vertical stratification and takes the values $\pm(1/2)$ at the different walls. In accord with experimental observations and linear theory for the stratified slot, we seek solutions, which are periodic in the vertical direction with dimensionless wavelength H where the width L of the slot is chosen to be the reference length. Here $H = H^*/L = 2\pi/\alpha$ is the dimensionless wave length: equivalently, α is the dimensionless vertical wave number of a periodic solution. τ_B is the dimensionless vertical temperature gradient, and Ra, Pr and γ are defined as usual, with β being the coefficient of thermal expansion of the liquid, and g is the constant gravitational acceleration.

The boundary value problem under consideration then takes the form:

$$\frac{1}{Pr}\frac{\partial \Delta\psi}{\partial t} + \frac{1}{Pr}\left(\frac{\partial\psi}{\partial y}\frac{\partial\Delta\psi}{\partial x} - \frac{\partial\psi}{\partial x}\frac{\partial\Delta\psi}{\partial y}\right) = -Ra\frac{\partial\theta}{\partial x} + \Delta^2\psi, \tag{2.1}$$

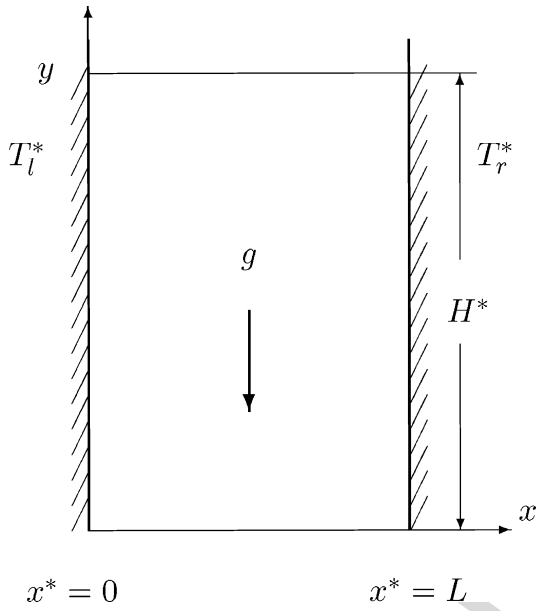

Fig. 1. Flow geometry: the asterisk refers to dimensional quantities. $T_l^* = T_0 + \tau_B^* y^*$, $T_r^* = T_0 + \delta T + \tau_B^* y^*$.

$$\frac{\partial\theta}{\partial t} + \left(\frac{\partial\psi}{\partial y}\frac{\partial\theta}{\partial x} - \frac{\partial\psi}{\partial x}\frac{\partial\theta}{\partial y}\right) - \tau_B\frac{\partial\psi}{\partial x} = \Delta\theta, \tag{2.2}$$

with boundary conditions

$$\begin{aligned} &\psi = \frac{\partial\psi}{\partial x} = 0, \quad \theta = -\frac{1}{2} \quad \text{for } x = 0, \\ &\psi = \frac{\partial\psi}{\partial x} = 0, \quad \theta = -\frac{1}{2} \quad \text{for } x = 1, \end{aligned} \tag{2.3}$$

and periodic conditions in vertical direction

$$\begin{aligned} &\psi(x, 0, t) = \psi(x, H, t), \qquad \psi_y(x, 0, t) = \psi_y(x, H, t), \qquad \psi_{yy}(x, 0, t) = \psi_{yy}(x, H, t), \\ &\psi_{yyy}(x, 0, t) = \psi_{yyy}(x, H, t), \qquad \theta(x, 0, t) = \theta(x, H, t), \qquad \theta_y(x, 0, t) = \theta_y(x, H, t). \end{aligned} \tag{2.4}$$

3. Difference scheme and algorithm

Define the following space time grid for the stream function ψ,

$$\psi_{ij}^n = \psi(x = h_x i,\ y = h_y j,\ t = \tau n),$$

for $i = -1, \ldots, M + 1$ and $j = -2, \ldots, N + 1$ and a staggered in time and space grid for the temperature θ,

$$\theta_{ij}^{n+(1/2)} = \theta(x = h_x[i - 0.5],\ y = h_y[j - 0.5],\ t = \tau[n + 0.5]),$$

for $i = 0, \ldots, M + 1$ and $j = 0, \ldots, N + 1$, where $h_x = L/M$, $h_y = H/N$ are the spacings in x- and y-directions, respectively, and τ is the time increment. We use grid that includes coordinate lines outside the domain to obtain symmetric second-order approximations of the boundary conditions for stream function. For instance, the boundary condition for ψ on the left wall $x = 0$, Eq. $(2.3)_1$, is approximated as

$$\psi_{0,j}^n = 0, \quad \psi_{-1,j}^n - \psi_{1,j}^n = 0 \cdot (2h_x) \quad \text{for } j = 0, \ldots, N - 1. \tag{3.1}$$

In a similar manner, the boundary conditions at the right wall, Eq. $(2.3)_2$ are approximated. As for the periodic conditions, Eq. (2.4), we imply the corresponding approximations in the solvers for periodic solutions. Since we are seeking periodic solutions of ψ and θ in the y-direction, it is worth noticing that a full period of the solution includes the horizontal grid lines from $j = 0, \ldots, N - 1$ for ψ, and $j = 1, \ldots, N$ for θ, respectively. Hence, the solutions on

the auxiliary horizontal grid lines outside the region are the periodic extensions of the solutions inside the period, for example, $\psi^n_{i,-2} \stackrel{\text{def}}{=} \psi^n_{i,N-2}$.

On the extended grid for ψ, we construct the second-order difference operators $C_x^{n+(1/2)}$ and $C_y^{n+(1/2)}$ for advective terms $-(\partial\psi/\partial x)(\partial\Delta\psi/\partial y)$ and $(\partial\psi/\partial y)(\partial\Delta\psi/\partial x)$ at time stage $(n+(1/2))$, respectively. Denote the difference approximation of the Laplacian differential operator as Δ_h and at the beginning of the internal iterations we use the standard second-order extrapolation of $\psi^{n+(1/2)}$, namely

$$\hat{\psi}_{ij}^{n+(1/2)} \stackrel{\text{def}}{=} \frac{3}{2}\psi_{ij}^n - \frac{1}{2}\psi_{ij}^{n-1}.$$

This amounts to three-level scheme, one more initial condition is imposed, namely $\psi^{-1} = \psi^0$. Now, the x- and y-derivatives of the vorticity $\Delta\psi^{n+(1/2)}$ can be approximated explicitly as follows

$$Q_{ij}^{n+(1/2)} = \frac{1}{2h_x}[(\Delta_h\hat{\psi}^{n+(1/2)})_{i+1,j} - (\Delta_h\hat{\psi}^{n+(1/2)})_{i-1,j}] \tag{3.2}$$

for $i = 1, \ldots, M-1$; $j = -1, 0, \ldots, N$.

$$P_{ij}^{n+(1/2)} = -\frac{1}{2h_y}[(\Delta_h\hat{\psi}^{n+(1/2)})_{i,j+1} - (\Delta_h\hat{\psi}^{n+(1/2)})_{i,j-1}], \tag{3.3}$$

for $i = 0, 1, \ldots, M$; $j = 0, \ldots, N-1$. Acknowledging the fact that the stream function ψ vanishes on the vertical boundaries and is periodic on the horizontal boundaries, we prove in [8] that if the advective operators are taken in the form,

$$\begin{aligned}
(C_x^{n+(1/2)}\psi^{n+(1/2)})_{ij} &= \frac{1}{2h_x}\left(P^{n+(1/2)}_{i+(1/2),j}\frac{\psi^n_{i+1j}+\psi^{n+1}_{i+1j}}{2} - P^{n+(1/2)}_{i-(1/2),j}\frac{\psi^n_{i-1j}+\psi^{n+1}_{i-1j}}{2}\right),\\
(C_y^{n+(1/2)}\psi^{n+(1/2)})_{ij} &= \frac{1}{2h_y}\left(Q^{n+(1/2)}_{i,j+(1/2)}\frac{\psi^n_{ij+1}+\psi^{n+1}_{ij+1}}{2} - Q^{n+(1/2)}_{i,j-(1/2)}\frac{\psi^n_{ij-1}+\psi^{n+1}_{ij-1}}{2}\right),
\end{aligned} \tag{3.4}$$

then they are antisymmetric in the sense that

$$\langle\psi^{n+(1/2)}, C_x\psi^{n+(1/2)}\rangle = 0, \quad \langle\psi^{n+(1/2)}, C_y\psi^{n+(1/2)}\rangle = 0,$$

with a properly defined scalar product for the set functions under consideration. For more details on the properties of these operators, see [8]. Here P and Q are evaluated on the staggered grid as follows

$$\begin{aligned}
P^{n+(1/2)}_{i+(1/2),j} &= \frac{1}{2}\left(P^{n+(1/2)}_{i+1,j} + P^{n+(1/2)}_{i,j}\right), \qquad P^{n+(1/2)}_{i-(1/2),j} = \frac{1}{2}\left(P^{n+(1/2)}_{i,j} + P^{n+(1/2)}_{i-1,j}\right),\\
Q^{n+(1/2)}_{i,j+(1/2)} &= \frac{1}{2}\left(Q^{n+(1/2)}_{i,j+1} + Q^{n+(1/2)}_{i,j}\right), \qquad Q^{n+(1/2)}_{i,j-(1/2)} = \frac{1}{2}\left(Q^{n+(1/2)}_{i,j} + Q^{n+(1/2)}_{i,j-1}\right),
\end{aligned} \tag{3.5}$$

which are of second-order of accuracy $O(h_x^2 + h_y^2 + \tau^2)$.

Hence, by the definitions of the advective operators $C_x^{n+(1/2)}$ and $C_y^{n+(1/2)}$, we are able to construct a difference approximation for Eq. (2.1) based on Arakawa-type (see [1]) scheme in the form:

$$\begin{aligned}
&\frac{1}{\tau Pr}\Delta_h(\psi_{ij}^{n+1} - \psi_{ij}^n) + \left[\frac{1}{Pr}(C_x^{n+(1/2)} + C_y^{n+(1/2)}) - (\Lambda_{x^4} + \Lambda_{y^4} + 2\Lambda_{x^2}\Lambda_{y^2})\right]\frac{\psi_{ij}^{n+1}+\psi_{ij}^n}{2}\\
&\quad = -Ra\frac{\theta^{n+(1/2)}_{i+1,j+1} - \theta^{n+(1/2)}_{i,j+1} + \theta^{n+(1/2)}_{i+1,j} - \theta^{n+(1/2)}_{i,j}}{2h_x} = F_{ij},
\end{aligned} \tag{3.6}$$

for $i = 1, \ldots, M-1$ and $j = 0, \ldots, N-1$. Here, central-difference approximations are used for different differential operators, which secure second-order of approximation in space and we denote the corresponding difference operators as Λ_{x^4}, Λ_{y^4}, $\Lambda_{x^2y^2}$, Λ_{xx}, Λ_{yy}.

It is well known, that using central differences for the first-order spatial derivatives in the advective terms, often leads to instability of the algorithm. However, if one takes special care (as we did here) to make central-difference

approximation strictly conservative, then the only problem that can appear is during the Gaussian elimination of the multidiagonal systems, because the main diagonal is not dominant. Yet, if the solver is carefully designed to use pivoting [3], then an instability of the elimination process cannot occur even for non-dominant main diagonal. Thus all the sources of divergence are eliminated. The central-difference scheme has a crucial advantage over the upwind schemes, in the sense that it does not have scheme viscosity. Thus, the calculations, even for very large Reynolds/Rayleigh numbers will have decent accuracy.

To solve (3.6) at each physical time step, we introduce an artificial time into the momentum Eq. (2.1) for the stream function, rendering it ultra-parabolic:

$$\frac{\partial\psi}{\partial s} = \frac{1}{Pr}\left[\frac{\partial\Delta\psi}{\partial t} + \left(\frac{\partial\psi}{\partial y}\frac{\partial\Delta\psi}{\partial x} - \frac{\partial\psi}{\partial x}\frac{\partial\Delta\psi}{\partial y}\right)\right] - \Delta\Delta\psi + Ra\frac{\partial\theta}{\partial x}. \tag{3.7}$$

In fact, one can add the artificial time directly in Eq. (3.6) and to conduct internal iterations (artificial time steps) until convergence is reached. Thus, a full step in physical time is obtained, for which the approximations of the non-linear terms and the boundary conditions are fully implicit with respect to the physical time.

Further on, we use factorization of the operator to be inverted in Eq. (3.6) that is based on operator splitting. In the specific implementation, we use the so-called second Douglass scheme [10] or the "scheme of stabilizing correction" (see, e.g. [18] for details). The advantage of the Douglas scheme is that it is absolutely stable even for non-commuting operators (at least as far as a linear problem is considered). Thus,

$$(E + A_y)\tilde{\psi} = \psi^{n,k} + L\psi^n - A_x\psi^n + \sigma F, \tag{3.8}$$

$$(E + A_x)\psi^{n,k+1} = \tilde{\psi} + A_x\psi^n, \tag{3.9}$$

where F is defined in Eq. (3.6) and the following notations are used for the operators involved,

$$A_y \stackrel{\text{def}}{=} -\frac{\sigma}{Pr\tau}\Lambda_{yy} - \frac{\sigma}{2Pr}C_y^{n+(1/2)} + \frac{\sigma}{2}\Lambda_{y^4}, \qquad A_x \stackrel{\text{def}}{=} -\frac{\sigma}{Pr\tau}\Lambda_{xx} - \frac{\sigma}{2Pr}C_x^{n+(1/2)} + \frac{\sigma}{2}\Lambda_{x^4},$$

$$L \stackrel{\text{def}}{=} -\frac{\sigma}{Pr\tau}\Lambda_{yy} - \frac{\sigma}{Pr\tau}\Lambda_{xx} + \frac{\sigma}{2Pr}C_x^{n+(1/2)} + \frac{\sigma}{2Pr}C_y^{n+(1/2)} - \frac{\sigma}{2}\Lambda_{x^4} - \frac{\sigma}{2}\Lambda_{y^4} - 2\sigma\Lambda_{x^2y^2}.$$

where σ is the increment with respect to the artificial time.

As shown in [8], the scheme for artificial time is absolutely stable for a "frozen" stream function, and gives a second-order approximation in real time, when the artificial time increment is $\sigma = (Pr\tau)^2$. In other words, although the scheme is first-order with respect to the artificial time, $O(\sigma)$, it is of second-order with respect to the real (physical) time and space, when the internal iterations converge, i.e. the truncation errors are of order of $O(\tau^2 + h_x^2 + h_y^2)$. Note, that the scheme has no artificial diffusion, because of the conservative approximation of the advective terms. The internal iterations begin from $\psi^{n,0} = \psi^n$ and are terminated when the following criterion is satisfied:

$$\frac{\max|\psi^{n,k+1} - \psi^{n,k}|}{\max|\psi^{n,k+1}|} < 10^{-7}.$$

The internal iterations represent, in fact, an evolution with respect to the artificial time. After they converge, the obtained function $\psi^{n,k}$ is set as the solution at the physical time level $(n + 1)$, namely ψ^{n+1}. Since the initial condition for this iterative process (artificial time transient) is close to the sought solution at the next time level, the number of iterations needed is, as a rule, small provided that the physical time increment is not unreasonably large. Clearly, the number of internal iterations decreases with the decrease of the real-time increment, τ. Conversely, if one chooses very large physical-time increments τ, then the number of iterations (artificial time steps) needed for convergence becomes very large. The optimal performance is achieved when the number of the internal iterations is kept around 11–80 in the sense that the real-time increment τ is still large enough, so that the process evolves reasonably quickly.

Turning to the temperature equation, we mention that the velocity components of the flow are computed from the values of the stream function ψ through the difference approximations of the definitive equalities $u = (\partial\psi/\partial y)$ and $v = -(\partial\psi/\partial x)$. Since a physical time step for ψ^n is executed before solving for $\theta^{n+(1/2)}$ (staggered in time scheme) we can consider ψ as known, and for the advective terms of θ we use the classical conservative approximation [14], which is akin to Arakawa [1] approximation for the convective terms of the momentum equations, but is much simpler for the heat equation.

Let us define the velocity components on the θ-grid as follows:

$$u^n_{i-(1/2),j} \stackrel{\text{def}}{=} \frac{1}{h_y}(\psi^n_{i-1,j} - \psi^n_{i-1,j-1}), \qquad u^n_{i+(1/2),j} \stackrel{\text{def}}{=} \frac{1}{h_y}(\psi^n_{i,j} - \psi^n_{i,j-1}),$$

$$v^n_{i,j-(1/2)} \stackrel{\text{def}}{=} -\frac{1}{h_x}(\psi^n_{i,j-1} - \psi^n_{i-1,j-1}), \qquad v^n_{i,j+(1/2)} \stackrel{\text{def}}{=} -\frac{1}{h_x}(\psi^n_{i,j} - \psi^n_{i-1,j}),$$

and the approximation of $\partial\psi/\partial x$ on the θ-grid is

$$G_{i,j} \stackrel{\text{def}}{=} \frac{\tau_B}{2h_x}(\psi^n_{i,j} - \psi^n_{i-1,j} + \psi^n_{i,j-1} - \psi^n_{i-1,j-1}).$$

Then, using the above notations, the difference operators of the advective terms the equation for θ (irrespective of its time stage) can be defined using the following formal operator notations:

$$(U\Lambda_x\theta)_{i,j} = \frac{1}{2h_x}(u^n_{i+(1/2),j}\theta_{i+1,j} - u^n_{i-(1/2),j}\theta_{i-1,j}), \qquad (V\Lambda_y\theta)_{i,j} = \frac{1}{2h_y}(v^n_{i,j+(1/2)}\theta_{i,j+1} - v^n_{i,j-(1/2)}\theta_{i,j-1}). \tag{3.10}$$

Finally, for the splitting scheme one has

$$\frac{\tilde{\theta} - \theta^{n-(1/2)}}{\tau} = \frac{1}{2}(\Lambda_{xx} - U\Lambda_x)[\tilde{\theta} + \theta^{n-(1/2)}] + (\Lambda_{yy} - V\Lambda_y)\theta^{n-(1/2)} + G_{ij} \tag{3.11}$$

$$\frac{\theta^{n+(1/2)} - \tilde{\theta}}{\tau} = \frac{1}{2}(\Lambda_{yy} - V\Lambda_y)[\theta^{n+(1/2)} - \theta^{n-(1/2)}], \tag{3.12}$$

in which $\Lambda_{xx} - U\Lambda_x$ and $\Lambda_{yy} - V\Lambda_y$ are inverted separately in two different half time steps.

Calculations for the coupled system begin from a given initial condition $\psi^{-1} = \psi^0 = f_0(x)$, $\theta^{1/2} = g_0(x)$, and are conducted until convergence in the periodic sense is reached in the stable cases, or until an exponential divergence is observed for the unstable cases.

The computations in this paper are done with different grid sizes, ranging from 80×80 to 320×320. The majority of the computations were performed on a 160×160 grid, with control checks for convergence using the finest grid. These checks show that our results on the 160×160 grid are accurate to within 1%. It goes beyond the frame of the present paper to report all the different exhaustive numerical experiments we did during validating the scheme.

4. Results and discussion

On the basis of linear analysis, Bergholz [2] found two different modes into which the bifurcation results: a traveling-wave solution (TW) and stationary-wave solution (SW). The results are quantitatively different for different Prandtl numbers and very often it is a mixed mode that takes place in the wake of the bifurcation. As mentioned in [2,4] the modes are better separated for large Prandtl numbers. For this reason, in this paper, we focus on the case $Pr = 10^3$ and examine the role of the wave number on the transition.

The parametric space of this problem is four-dimensional and it is impossible to cover even a small fraction of the important cases in a single paper. In order to stay within reasonable limits, we restrict ourselves to only two values of stratification parameter $\gamma = 2$ and $\gamma = 8$. For the first one, only a traveling mode is expected to exist, while for the second, the stationary mode is first to onset and then for higher Ra, once again a TW mode can appear.

Here is to be mentioned that a non-linear bifurcation can be much more complex a phenomenon than a linear one, in the sense that for a given set of parameters one can have the so-called "hanging-bifurcation" not connected with a linear eigen-value. A non-trivial solution can appear for sufficiently large initial condition for set of parameters for which the linear theory predicts that the main motion is stable. An absolutely conservative scheme as the one developed here can be a powerful tool in investigating the actual mode of bifurcation. For all different sets of parameters we used a very small initial perturbation and increased the Rayleigh number until we got an increasing amplitude. This answers the question of the linear instability. When we started the evolution from a finite-amplitude disturbance, we succeeded to get a non-trivial solution for a lower Rayleigh number when all other parameters are kept the same. The

thorough investigation of this phenomenon requires a lot of numerical experiments with different grid sizes and time increments in order to prove that this is not an effect connected with the approximation of the scheme. It goes beyond the framework of the present contribution and will be investigated separately in the future. In this paper, we focus on the properties of the solution near the threshold of the linear instability.

Our scheme allows us to investigate the issue of the most dangerous mode. In linear-stability theories, the most dangerous mode is defined as the mode which has the fastest time increment. By maximizing the imaginary part of the solution of the dispersion equation for the frequency, one gets the most dangerous wave number. In a numerical approach, there is no explicit formula for the most dangerous mode. In fact, the wave number is predetermined by the size of the vertical box, H chosen in each particular case. The amplitude of the numerically obtained non-linear wave for a given H can serve as a rough indicator of the propensity of the wave to grow, but there is no whatsoever rigorous connection between the terminal amplitude of the wave and the growth rate at the initial stage.

To find the non-trivial solution when it exists, we construct the initial condition as a main part, which is the solution of the one-dimensional version of the equations and a small initial perturbation for the stream function in one or two points. We do not impose initial perturbation on the temperature field. We have taken different values for the perturbation, and found that the threshold in Ra for which a non-trivial perturbation is obtained, does not depend significantly on the amplitude of the initial disturbance.

4.1. Stationary-wave (SW) mode, $\gamma = 8$

Begin with the case of relatively larger stratification parameter $\gamma = 8$ when the bifurcation yields to a stationary-wave. The sequence of panels in Fig. 2 shows the particular shape of the solution we obtain for different prescribed values of the wave length (size of the vertical box in calculations). For wave lengths $H < 1.2$, the solution of the two-dimensional problem coincides with the one-dimensional solution, i.e. no perturbation develops. The smallest value of the vertical size of the box for which non-trivial perturbation takes place is $H = 1.25$. Then, we increase the wave length and we are still able to a get solution. Fig. 2 demonstrates the dependence of the solution on the selected wave length. The non-linearity makes the main part of the vortex increase, while the changes are localized roughly in the same regions for the solution with $H = 1.5$. This pattern is preserved up to $H = 2.5$ and then for $H = 2.75$ two waves of length $H = 1.375$ appear. Respectively, a box of length $H = 3$ harbors two complete waves of length $H = 1.5$. Note, that in the cases with larger H we took larger number of points in vertical direction, so the overall approximation is roughly the same.

Clearly, one can expect the scenario to be repeated with the increase of H. Indeed, we see in Fig. 2(h) that increasing the vertical dimension of the box to $H = 4$ merely results in stretching the vortices and we still get just two complete

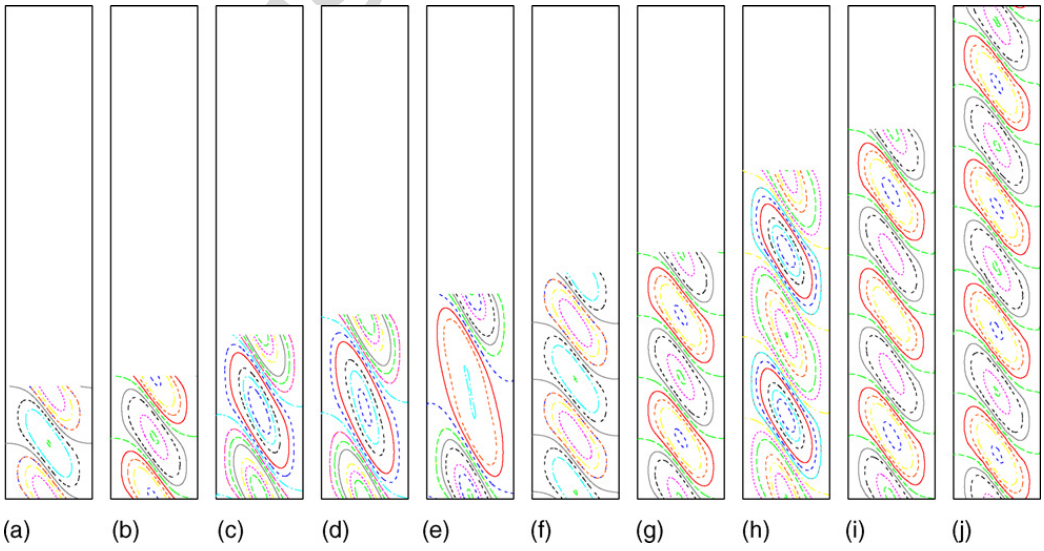

Fig. 2. Stationary mode for different wave lengths: (a) $H = 1.375$; (b) $H = 1.5$; (c) $H = 2$; (d) $H = 2.25$; (e) $H = 2.5$; (f) $H = 2.75$; (g) $H = 3$; (h) $H = 4$; (i) $H = 4.5$; (j) $H = 6$.

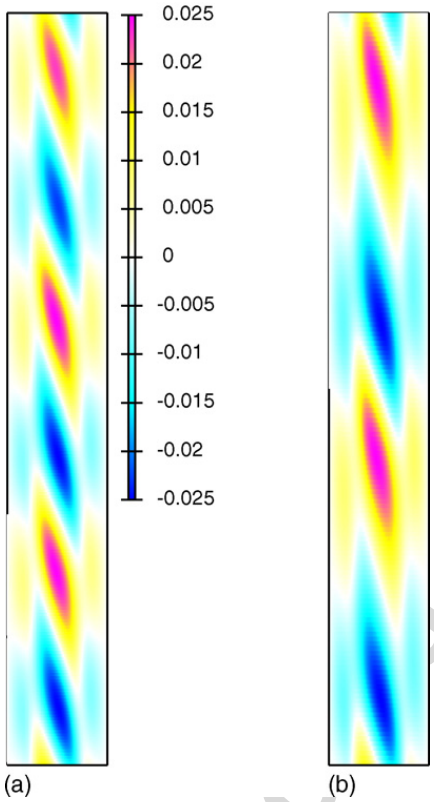

Fig. 3. Perturbation of the temperature in the SW mode: (a) concatenated patterns for four waves with $H = 1.5$ and (b) concatenated patterns for three waves with $H = 2.25$.

waves of length $H = 2$. The crucial experiment is the next panel, Fig. 2(i) for $H = 4.5$ which shows that three complete waves of length $H = 1.5$ appear there, rather than two complete waves of length $H = 2.25$ of the type shown in Fig. 2(d). This can be considered as a non-linear test for which is the more dangerous mode: it is the shorter one in this case. Fig. 2(j) shows the solution for size of the vertical box $H = 6$. Now, one gets four complete waves of length $H = 1.5$ rather than three complete waves of length $H = 2$. Clearly, the shorter wave is more dangerous not only than the wave with length $H = 2.25$, but also than the wave of length $H = 2$. If it could be of any indication we mention here that the shorter wave $H = 1.25$ has significantly smaller amplitude than $H = 1.5$. According to the handwaving arguments, this can mean that it is less dangerous. Hence, we get $H = 1.5$ as the most dangerous wave which is in very good agreement with [2].

In Fig. 3, where we show for completeness, the solution for the temperature obtained with $H = 1.5$ and $H = 2.25$. We concatenate the waves in order to compare them. In the left panel, three wave lengths are concatenated, while in the right panel, only two wave lengths are matched to each other. We mention that the solution in the right panel can never be obtained from the simulations, because the shorter wave is which always takes place for box $H = 4.5$.

We mention also that in the case of the temperature, the boundary layer that forms near the boundaries becomes visible. As shown in [15], the thickness is of order of γ^{-1} and for this reason it is not visible in the plots for the stream function.

4.2. Traveling-wave (TW) mode, $\gamma = 2$

Consider now the case $\gamma = 2$, when the one-dimensional stationary solution is unstable to TW modes. This means that the perturbation is a function of time: a pattern that propagates along the vertical axis. The most dangerous wave number predicted from the linear theory [2] is $\alpha \approx 2.55$ ($H = 2\pi/\alpha \approx 2.4$) and the critical Rayleigh number is in the vicinity of $Ra = 250,000$. For this wave length, we did indeed find a non-trivial solution, which is traveling-wave. Several snapshots in time of the solution are presented in Fig. 4. The upper panels show the perturbation of the stream function, while the lower panels present the temperature perturbation.

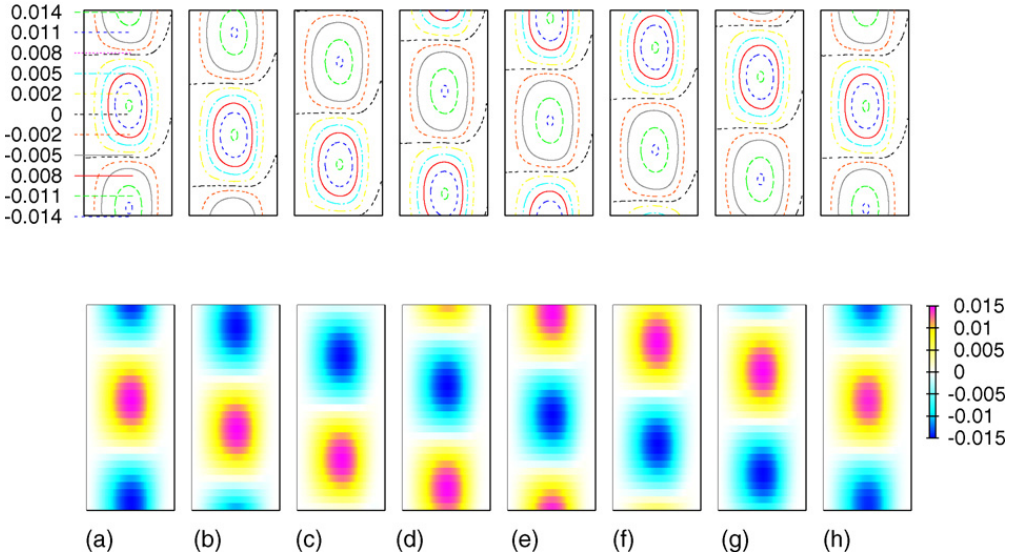

Fig. 4. The perturbations for $Pr = 1000$, $\gamma = 2$, $Ra = 2.4 \times 10^5$, $H = 2.4$, and 160×160 grid: (a) $t = 0$; (b) $t = 9\tau$; (c) $t = 18\tau$; (d) $t = 27\tau$; (e) $t = 36\tau$; (f) $t = 45\tau$; (g) $t = 54\tau$; (h) $t = 63\tau$.

We found that the flow is a traveling-wave, which takes 63 time steps to clear distance equal to its length. The traveling-wave is the real part of the following function:

$$F(x)\,\mathrm{e}^{i\Omega t+\alpha y}, \quad c = \frac{\Omega}{\alpha} = \frac{H}{T},$$

where $F(x)$ is a complex function of the horizontal coordinate, c is the phase speed of the traveling-wave, and T is the time period of the wave. Now, from the above-presented data we find that $T = 63\tau$. In order to calculate the phase speed, we mention that in this particular case we took $\tau = 2\pi/(320 \cdot Pr) = 2\pi/320,000$ guided by consideration of stability and approximation (note that Prandtl number is very large). This particular choice means that we have 320 time stages in a single period of the so-called convective time (time rescaled by Prandtl number). Thus

$$\Omega = \frac{2\pi}{T} = \frac{2\pi}{63\tau} = \frac{320,000}{63} \approx 5079,$$

which is in good agreement with [2], where the frequency of the traveling mode for $Ra = 300,000$ is 6120 (see [4] for the comparison between the dimensionless variables of [2] and present work). The quantitative investigation of the traveling mode require a large scale numerical experiment that goes beyond the scope of the present work devoted to the development of a new numerical tool.

Next, we address the issue of most dangerous mode for the TW. We present in Fig. 5 the evolution of the solution in time for wave of length $H = 1.75$. The frequency of this wave is higher (period is shorter). We get repeating patter at $T = 44\tau$. If $H = 1.75$ was a dangerous mode, then increasing the length twice should bring two complete solutions of length $H = 1.75$. The computations with $H = 3.5$ are shown in Fig. 6 and it is clearly seen that a wave with length $H = 3.5$ takes place, not the wave $H = 1.75$. This means that $H = 1.75$ is not more dangerous than $H = 3.5$. In the latter case the period is $T = 85\tau$.

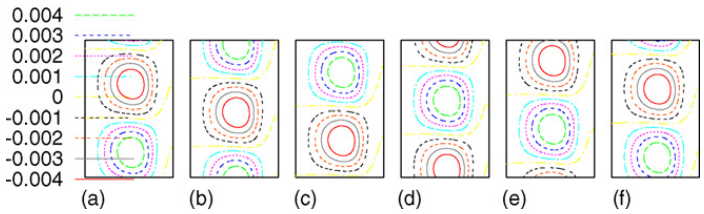

Fig. 5. The perturbations for $Pr = 1000$, $\gamma = 2$, $Ra = 2.6 \times 10^5$, $H = 1.75$, and 80×160 grid: (a) $t = 0$; (b) $t = 9\tau$; (c) $t = 18\tau$; (d) $t = 27\tau$; (e) $t = 36\tau$; (f) $t = 45\tau$; (g) $t = 54\tau$.

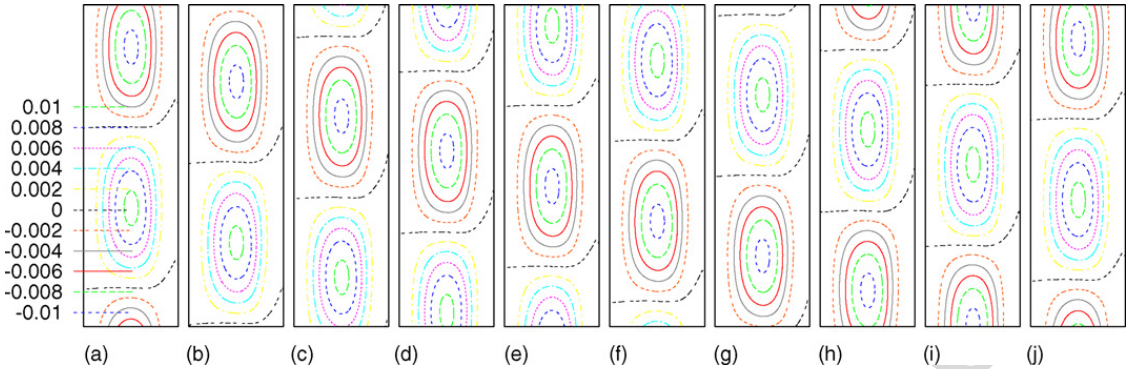

Fig. 6. The perturbations for $Pr = 1000$, $\gamma = 2$, $Ra = 2.6 \times 10^5$, $H = 3.5$, and 80×320 grid: (a) $t = 0$; (b) $t = 9\tau$; (c) $t = 18\tau$; (d) $t = 27\tau$; (e) $t = 36\tau$; (f) $t = 45\tau$; (g) $t = 54\tau$; (h) $t = 63\tau$; (i) $t = 72\tau$; (j) $t = 81\tau$.

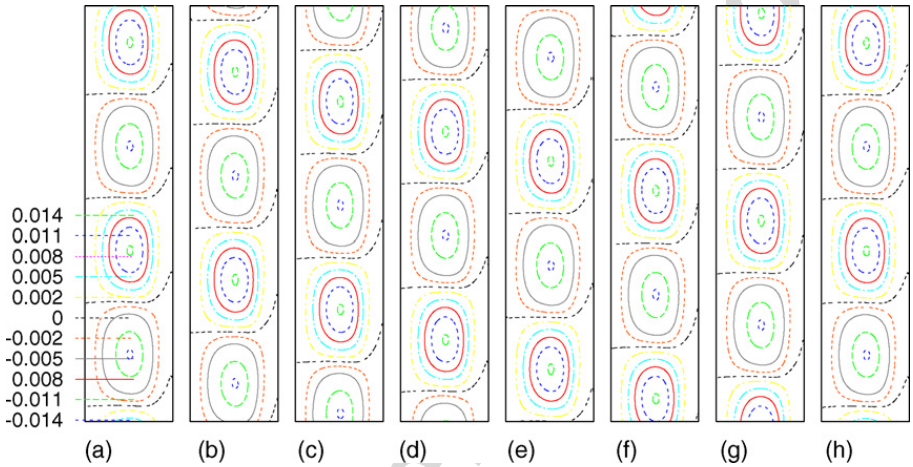

Fig. 7. The perturbations for $Pr = 1000$, $\gamma = 2$, $Ra = 4.8 \times 10^5$, $H = 4.8$, and 80×320 grid: (a) $t = 0$; (b) $t = 9\tau$; (c) $t = 18\tau$; (d) $t = 27\tau$; (e) $t = 36\tau$; (f) $t = 45\tau$; (g) $t = 54\tau$; (h) $t = 63\tau$.

Table 1
Periods and phase speeds of the three observed TW modes

H	T	c	Ra ($\times 10^5$)
1.75	8.6350×10^{-4}	2026.6	2.6
2.4	1.2364×10^{-3}	1941.2	2.4
3.5	1.6681×10^{-3}	2098.2	2.6

Finally, we computed the case $H = 4.8$ which is presented in Fig. 7. Now it is clearly seen that the wave of length $H = 2.4$ is more dangerous, because it fills the whole box with two periods. This means that $H = 2.4$ is more dangerous than $H = 4.8$, which is in good qualitative agreement with [2] where, the linear analysis identified the mode $H = 2.4$ as most dangerous. The period in the last case is exactly the same as for $H = 2.4$, and it is $T = 63\tau$. Note that in this case we count as a full period the time needed to establish exactly the same wave pattern, not the time needed for the top vortex to travel the whole box.

The above results show that the dimensionless period differs significantly with the wave length, but the phase speed is virtually constant as shown in Table 1. It is seen that the different waves have different time periods, but the phase speed are close to each other. The phase speed of wave $H = 2.4$ is somewhat lower, because the Rayleigh number is smaller.

5. Summary

In this paper, we have investigated the bifurcation and emerging of a secondary circulation in the flow of a horizontally and vertically stratified fluid in a finite slot for supercritical Rayleigh numbers, Ra. Depending on the value of the

stratification parameter, γ, the main flow is unstable either to traveling (TW), or stationary (SW) wave modes. A large Prandtl number, $Pr = 1000$ is considered when the different instability modes are widely separated in the domain of variation of γ.

To this end, we have created an absolutely stable implicit difference scheme based on operator splitting of the parabolic system obtained after an artificial time derivative is added in the unsteady equation for the stream function. A special attention is paid to the approximation of the non-linear advective terms (a modification of Arakawa scheme for the implicit case), that makes the splitting scheme for artificial time stepping absolutely stable, provided that coefficients involving vorticity function at a given time stage of the physical time are thought of as "frozen". The time levels of the physical time are staggered as are the space grids for ψ and θ. This enables one to compute the unknown functions in an appropriate sequence without losing the second-order approximation for the coupled solutions both in time and space. The issues of implementation of the algorithm involving internal iterations are tackled and results are obtained for both SW and TW.

The results for the physical properties of the bifurcation can be summarized as follows:

(i) The non-linear two-dimensional solutions are in general agreement with the linear stability calculations of [2] in the sense that we observe bifurcation near the same values of Ra and γ, as predicted by linear theory.
(ii) When the vertical size of the domain is increased, more than one wave length can be observed. In such a case, the most dangerous wave takes place, and the most dangerous wave in the non-linear computations seems to agree with the most dangerous wave of the linear theory. What is achieved here beyond the linear theory is to find the actual amplitude and shape of the perturbations for different wave lengths.

References

[1] A. Arakawa, Computational design for long-term numerical integration of the equations of fluid motion: two-dimensional incompressible flow. Part I, J. Comput. Phys. 1 (1966) 119–143.
[2] R.F. Bergholz, Instability of steady natural convection in a vertical fluid layer, J. Fluid Mech. 84 (1978) 743–768.
[3] C.I. Christov, Gaussian elimination with pivoting for multidiagonal systems, internal report 4, Technical Report, University of Reading, 1994.
[4] C.I. Christov, G.M. Homsy, Nonlinear dynamics of two dimensional convection in a vertically stratified slot with and without gravity modulation, J. Fluid Mech. 430 (2001) 335–360.
[5] C.I. Christov, J. Pontes, Numerical scheme for Swift–Hohenberg equation with strict implementation of Lyapunov functional, Math. Comput. Model. 35 (2002) 87–99.
[6] C.I. Christov, A. Ridha, Splitting scheme for iterative solution of bi-harmonic equation. Application to 2D Navier–Stokes problems, in: I. Dimov, Bl. Sendov, P. Vasilevskii (Eds.), Advances in Numerical Methods and Applications, Proceedings of the 3rd International Conference on Numerical Methods $O(h^3)$, Sofia, Bulgaria, August, World Scientific, Singapore, 1994, pp. 341–352.
[7] C.I. Christov, A. Ridha, Splitting scheme for the stream-function formulation of 2D unsteady Navier–Stokes equations, C. R. Acad. Sci. Paris IIb (1995) 441–446 t. 320.
[8] C.I. Christov, X.-H. Tang, An operator splitting scheme for the stream-function formulation of unsteady Navier–Stokes equations. Int. J. Numer. Meth. Fluids, 10.1002/fld.1285.
[9] S.D. Conte, R.T. Dames, On an alternating direction method for solving the plate problem with mixed boundary conditions, J. ACM 7 (1960) 264–273.
[10] J. Douglas, On the numerical integration of $\partial^2 u/\partial x^2 + \partial^2 u/\partial y^2$ by implicit methods, SIAM J. 3 (1955) 42–65.
[11] J.W. Elder, Laminar free convection in a vertical slot, J. Fluid Mech. 23 (1965) 77–98.
[12] A. Farooq, G.M. Homsy, Linear and nonlinear dynamics of a differentially heated slot under gravity modulation, J. Fluid Mech. 313 (1996) 1–38.
[13] A.E. Gill, A. Davey, Instabilities of buoyancy-driven system, J. Fluid Mech. 35 (1969) 775–798.
[14] G.I. Marchuk, Methods of Numerical Mathematics, vol. 4, Springer-Verlag, 1975.
[15] N.C. Papanicolaou, C.I. Christov, A Galerkin spectral method for thermo-convection boundary value problem, Neural Parallel Sci. Comput. 10 (2002) 339–354.
[16] X.-H. Tang, C.I. Christov, An operator splitting scheme for biharmonic equation with accelerated convergence, in: I. Lirkov, S. Margenov, J. Wasniewski (Eds.), Large Scale Scientific Computating, Lecture Notes in Computer Sciences, 3743, Springer-Verlag, 2005, pp. 380–387.
[17] X.-H. Tang, C.I. Christov, A multiunit ADI scheme for biharmonic equation with accelerated convergence, Int. J. Computat. Sci. Eng., in press.
[18] N.N. Yanenko, Method of Fractional Steps, Gordon and Breach, 1971.